This paper will be published in the Proceedings of
the 12th International Congress on the Deterioration and Conservation of Stone,
New York, 22-25 October 2012

Compatibility of Roman cement mortars with gypsum stones and anhydrite mortars: The example of Valère Castle (Sion, Switzerland)

C. Gosselin[1*], F. Girardet[2], S.B. Feldman[3]

[1] Laboratory of Construction Materials, Ecole Polytechnique Fédérale de Lausanne, CH-1015 Lausanne, Switzerland, christ.gosselin@gmail.com
[2] Rino Sarl, CH-1807 Blonay, Switzerland, fred.girardet@bluewin.ch
[3] Active Minerals International LLC, Cockeysville, USA, s.feldman@activeminerals.com

1. Abstract

Durable and reversible restoration of stones and historical mortars is a major concern to those interested in conservation of historical structures and contemporary practices of restoration are continuously revisited with the help of the technical and scientific researches. However, the historical feedback on repairing techniques recently showed that Roman cements (RC), developed and widely used through the XIXth Century, were particularly well-adapted to repair historical masonries. The current article presents a case study of RC mortars applied on gypsum stones and historical anhydrite mortars, both soluble and known to be sensitive to the chemical compatibility with hydraulic binders. Mineralogical analysis of samples from the basilica Notre Dame de Valère (Sion, Switzerland) shows that late XIXth C. RC joints and renders have perfectly lasted in contact with the structural gypsum stones and anhydrite mortars from the XIIIth C. Results from XRD and SEM work suggest that the present RC was produced at a temperature high enough to form significant amounts of β-C_2S and C_2AS, remaining unreacted after very long term hydration. The extent of C_2S hydration is notably reduced due the precipitation of silica gel, a carbonation product, at the boundary of the cement grains. The high capillary porosity developed during hydration is homogeneously distributed, enhancing the transport properties. These conclusions were supported by complementary observations. First, elemental mapping through the strong RC /anhydrite mortars interface does not indicate any accumulation of sulfate salts at the boundary. Additionally, in contrast to the RC mortars, the rapid expansion and degradation of grey Portland cement mortars was observed, confirming the limitations of the latter applied on gypsum stones.

Keywords: Roman cement, gypsum stone, anhydrite mortars, microstructure, compatibility

* Now at Geotest, Le Mont-sur-Lausanne, Switzerland, christophe.gosselin@geotest.ch

2. Introduction

The basilica Notre Dame de Valère (also called Castle of Valère) is part of a fortified village built in the XIIth C., on the top of a hill overlooking the city of Sion. In 1877, the cantonal Great Council called upon the Government to report on the ownership of the feudal castles of the canton and the measures for their conservation. A major restoration campaign of the Valère Castle was conducted between 1892 and 1902 under the supervision of the Swiss Society for the Conservation of Historic Buildings. The work was led by the Office Kalbermatten under the direction of the architect Theophile van Muyden [1].

The masonry is composed of different types of local stones (calcareous, tuff and gypsum stones). Two varieties of local gypsum stones were used (white gypsum stones, i.e. alabaster, and yellowish gypsum stones containing sand) for both ashlar masonry and sculpted ornamentations in areas unexposed to rain. The protection of the gypsum stones from the rain led to their relatively good state of conservation despite their high solubility (2 g/l). However, the dissolution of gypsum stones in areas exposed to rain, and the subsequent release of sulphate ions can lead to major conservation concerns related to their compatibility with the different hydraulic binders used for the joints, the structural and decorative elements [2]. This article discusses the specific case of restoration joints made of XIXth C. Roman cement based mortars.

Several types of mortars are present on the façades, according to the period of construction and restoration of the building. Six types of mortars were identified as shown in Table 1. The present study focuses on the compatibility of the XIXth C. Roman cement mortars (types 3 and 4) versus that of the Portland cement mortars (type 5) with the gypsum stones and the anhydrite mortars (type 2).

Type of mortar	Description
Type 1	Original *pietra rasa* lime mortar (XIIIth C.), white
Type 2	Original anhydrite mortars (XIIIth C.), pinkish
Type 3	Restoration Roman cement mortars (1896), thin pointing mortar, concave (spatuled), covering the original lime mortar, beige to greyish
Type 4	Restoration Roman cement mortars (1898), thick and extruded repointing mortars, beige to greyish
Type 5	Restoration Portland cement mortars (end of the XIXth C., as Type 3 and 4), cast mortar to repair elements made of gypsum stone, dark grey
Type 6	Restoration hybrid mortar (hydraulic lime and white cement) (1997-2003), repointing deep joint, white

Table 1 Types of original and restoration mortars identified on the façades

The use of anhydrite ($CaSO_4$) or gypsum ($CaSO_4.2H_2O$), commonly with lime, to produce joint, precast or render mortars is reported in several historical buildings from the Ancient Egypt period (e.g. Cheops and Unas pyramids [3]) to more recent periods of decorative architecture [4,5], through the Medieval period in Europe (e.g. North German [6] and French cathedrals [7]). The choice of anhydrite or gypsum was usually motivated by the appearance (colour, texture) of hardened calcium sulphate based mortars close to that of lime mortar. Mixtures of lime and gypsum (so-called *estrich gyps*) are also reported in German monuments.

Roman cement is a hydraulic binder developed in Europe in the early XIXth C. and widely used both for civil engineering and architectural restoration applications. Several studies in the field of stone and mortars conservation have revisited and highlighted the unique and lasting properties of this material to repair historical masonries [8-10]. Roman cements are sometimes called “Natural” cement, in contrast to artificial Portland cements (i.e. co-ground with added gypsum) in some countries such as France [11] or USA [12]. This family of hydraulic binder results from the calcination of naturally occurring limestones rich in clay minerals below the sintering point (800-1000°C) and the grinding of the burnt material to a fine cement. A typical shaft kiln was used during the early production of these cements. Roman cement has been produced from the 1830’s in the North of Switzerland (Solothurn and Aarau) and increasingly used throughout the XIXth C. The development of the Swiss railway network in the 1850’s required rapid materials for the lines construction and contributed to the promotion of the Swiss Roman cements. The annual production of cement reached 60 t in

1851. However, despite of the quality of the local raw materials, the Swiss production could not compete with the other European producers and the importation of Roman cement from France increased from 1857 (with an import of 35000 tons recorded in 1876). The two main production sites were Vicat (Grenoble) and Pavin de Lafarge (Virieu le Grand, Isère) [13].

3. Samples and methods

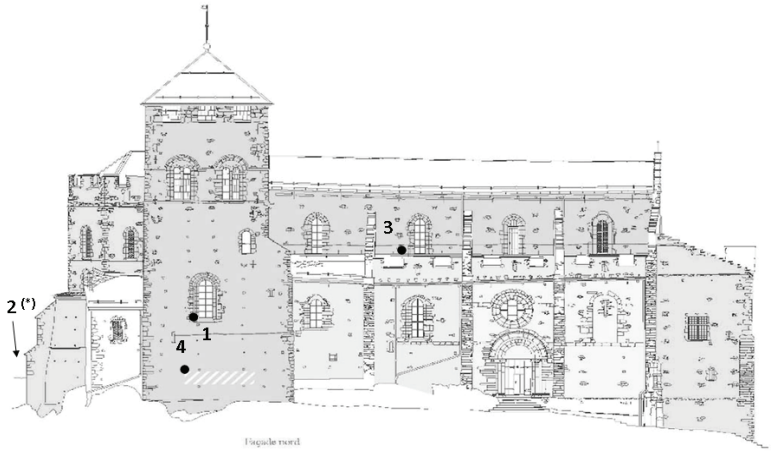

Figure 1 View of the Northern façade of the Valère castle and samples location (after Amsler and Gagliardi)

Figure 1 gives the location of the mortars samples from the Northern façade of the church. The mortar 2 was sampled from the Eastern façade (annex buildings in ruins not illustrated in Figure 1). Figure 2 gives detailed views (cross sections) of the four samples (three Roman cement mortars and one Portland cement mortar) used for the microstructural characterisation (SEM and XRD). Scanning Electron Microscopy (SEM, Philips Quanta 200) was used to study the microstructure of the mortar samples. The samples were impregnated with epoxy resin and polished to obtain cross sections. The microanalysis of phases and elemental mappings were done with Energy Dispersive Spectroscopy (EDS, Bruker AXS Quantax). XRD analysis was done on sieved mortar samples using an X'Pert Pro PANAlytical diffractometer (Cu tube, λ=1.54 Å). The Rietveld method was applied for the crystalline phase quantification.

4. Results

1. Macroscopic observations of the mortars samples

The Portland cement mortar (sample 1) was applied to replicate a column of a window frame originally made of white gypsum stone. From Figure 2, the bulk mortar sample looks beige (most probably due to the superficial atmospheric carbonation), but the cross section prepared for microscopy reveals a grey matrix. The bulk mortar is dense and no specific degradation pattern is observed. The outer subsurface (exposed to the environment) is notably distinguished by a colour slightly switching from grey to light beige. The dissolution of the gypsum stone substrate, appearing yellow after epoxy resin impregnation, is well advanced and a high amount of matter was lost during the sample preparation. A thick reaction interface is marked at the mortar/stone interface (top right image of Figure 2).

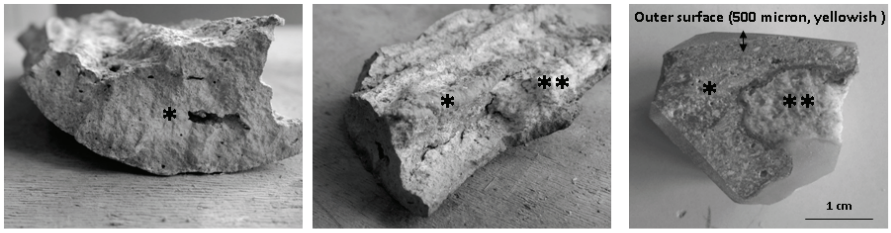

Sample 1
Portland cement mortar (*) cast on original gypsum stone (**)
The cross section shows a dense and greyish matrix of mortar. The content of fine sand is relatively low. The outer surface is slightly yellowish. The gypsum stone is strongly dissolved and the interface mortar/stone is relatively thick.

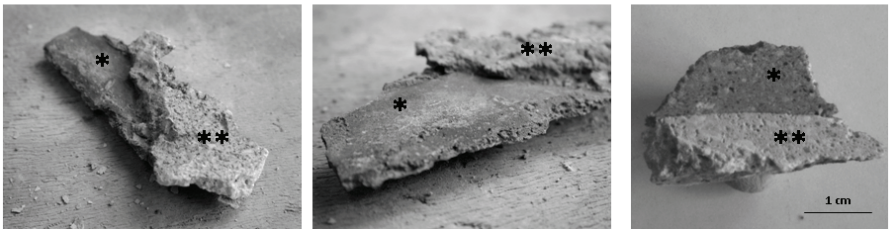

Sample 2
Roman cement mortar (*) applied on original anhydrite mortar (**)
The cross section shows a dense and greyish matrix of Roman cement mortar, with a low content of fine sand. The dense anhydrite mortar has light pink colour. Both mortars are mechanically bound by a strong and thin interface.

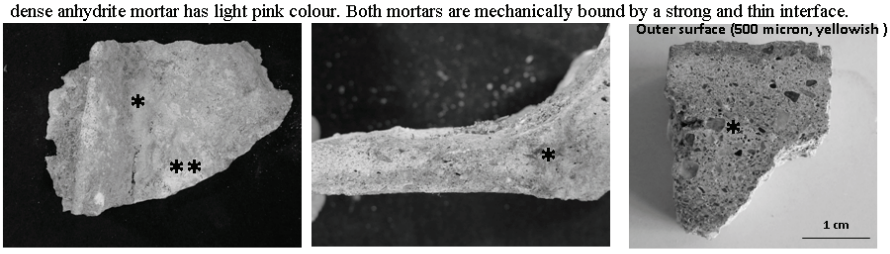

Sample 3
Roman cement repointing mortar (*) covering the original gypsum stone (**).
The cross section shows a dense and greyish matrix of mortar. The outer surface (0.5 mm) is yellowish.

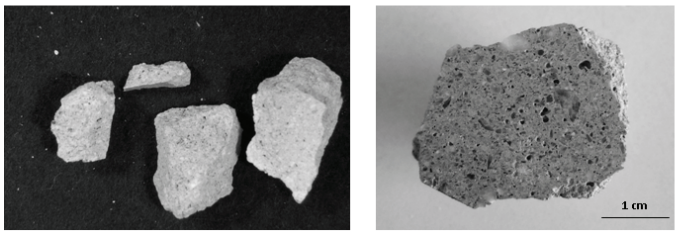

Sample 4
Roman cement mortar cored from a thick joint.
The cross section shows a greyish matrix of mortar. The sand content is relatively high. Some macropores are (entrained air from mixing) are evenly distributed through the section.

Figure 2 Photographs and description of the mortars samples

The bulk Roman cement samples have different colours according to their location and application. Sample 2 was applied as a thin render on the original XIIIth C. anhydrite mortar. While the matrix of the cement mortar is dark grey (outer surface and bulk), that of the anhydrite mortar is pinkish and contains coarse white inclusions. The two mortars are strongly bound by a very thin interface.

Sample 3 is a thick joint partly covering and profiling an adjacent a gypsum stone (some fragments of stone remains visible in Figure 2). This sample was removed from the façade and collected on the first roof of the Northern façade. The outer surface of the sample looks beige but the cross section shows a dark grey matrix, comparable to the Portland cement sample 1. The cross section also reveals the formation of a thin (500 micron) and yellowish subsurface that is exposed to the atmosphere. This specific layer was already reported in French [9] and Austrian [8] samples but its origin (atmospheric oxidation, footprint of organic product, such as wax, originally used for technical or aesthetical purposes,…) is not fully

understood. The mortar is composed of coarse aggregates. Micropores from mixing are randomly distributed through the matrix.
Sample 4 was collected from a core in a thick joint. The light colour (beige) of the bulk mortar remains even after the cross section preparation and this mortar is notably lighter than the previous ones. Figure 2 shows a dense matrix despite a high macroporosity formed during the mixing.

2. XRD analysis on the mortars

The crystalline composition of the RC mortars, suggested by the best-fit values of the Rietveld analysis, is given in Table 2. The nomenclature of cement chemistry (C=CaO, S= SiO_2, A= Al_2O_3, F= Fe_2O_3, $\underline{C}$=CO_3, H=H_2O) is used for given phases in this table.

Origin of phase	Phase	Sample 1	Sample 2	Sample 3	Sample 4
(1)	Microcline $KAlSi_3O_8$	1.2	4.2	2.0	4.2
	Albite $NaAlSi_3O_8$	14.3	15.0	5.7	16.4
	Clinochlore $(Mg,Fe)[(OH)_8AlSi_3O_8$	3.7	5.6	3.5	4.7
	Muscovite $K_2Al_4[(OH,Fe)AlSi_3O_{10}$	4.0	3.6	5.0	3.0
	Actinolite $Ca_2(Mg,Fe)_5Si_8O_2.2(OH)_2$	2.2	2.5	1.6	1.6
(2)	Quartz SiO2	17.7	13.9	16.8	13.0
(3)	Periclase MgO	-	-	1.4	-
	Tileyite $Ca_5(Si_2O_7)(CO_3)_2$	-	-	1.4	-
	Belite β-2CaO.SiO_2 or β-C_2S	10.7	2.0	26.3	-
	Alite 3CaO.SiO_2 or C_3S	7.4			
	Gehlenite 2CaO.Al_2O_3.SiO_2 or C_2AS	3.0	9.5	2.9	12.4
	Ferrite $Ca_2(Al,Fe)_2O_5$ or C_4AF	0.7	-	2.6	-
(4)	Calcite $CaCO_3$ or $C\underline{C}$	9.0	26.2	15.3	35.4
(5)	Vaterite $CaCO_3$	-	1.8	0.8	1.0
	Aragonite $CaCO_3$	-	6.2	-	6.2
(6)	Portlandite $Ca(OH)_2$ or CH	7.5	-	1.7	-
(7)	Gypsum $CaSO_4.(H_2O)2$	3.6	8.4	3.4	2.0
	Ettringite $Ca_6(Al(OH)_6)_2(SO_4)_3(H_2O)_{26}$	4.4	-	8.4	-

Table 2 Quantitative XRD of the mortar samples : (1) from aggregates, (2) from aggregates or anhydrous cement, (3) from anhydrous cement, (4) from aggregates, anhydrous cement or carbonation product, (5) carbonation products, (6) hydration products, (7) hydration products (Ett.) or reaction products with external sulfate

Table 2 discriminates different sources of crystalline phases. Some common minerals such as microcline, albite, clinochlore, muscovite and actinolite originate from the local sand and were identified in various amounts in all samples. Quartz and calcite could also be attributed to the aggregate fraction in the Portland cement mortar (sample 1) but part of these phases can be also attributed to residual remnants of Roman cements [14].

Despite the long time of contact with moisture on the façades, the roman cement samples (2 to 4) contain unreacted phases. The β polymorph of belite is identified in different amounts. In the typical range of calcination temperature of roman cement, α'-2CaO.SiO_2 dominates and hydrates afters few weeks of contact with mixing water and moisture [15]. When the calcination temperature becomes higher, β-2CaO.SiO_2 can form but is less reactive than the α' polymorph. By achieving higher temperature in the kiln, more alumina from the raw clay minerals becomes available to form gehlenite (2CaO.Al_2O_3.SiO_2), a low reactivity phase. Note that β-belite and gehlenite are also identified in the Portland cement sample. Indeed β-

belite is a secondary reactant in Portland cements much less reactive than tri-calcium silicate $3CaO.SiO_2$, the main reactive phase responsible for the strength development.
Gehlenite, which is sparingly present in contemporary Portland cements and has been identified in early PC (XIXth C.) [16], is said to be suggestive of underburnt Portland cement (usually calcined above 1400°C) [17].

As abovementioned, the presence of calcite can be attributed to the mortar sand but also to the carbonation of cement hydration products. Both Portland and Roman cement, and tri- and dicalcium silicate, respectively, hydrate to form calcium silicate hydrate (C-S-H) and calcium hydroxide (CH). Remaining calcium hydroxide was identified in samples 1 and 3 (Table 2) but its carbonation under atmospheric conditions (e.g., CO_2, wetting/drying cycles) led to the precipitation of calcite and other metastable calcium carbonate polymorphs (aragonite and vaterite), particularly in the Roman cement samples. The metastable $CaCO_3$ polymorphs transform to stable calcite by dissolution-precipitation reaction but can coexist in dry environment [18], which is the case of the Northern façade of the present structure. Note that the C-S-H phase could also be subject to carbonation and comparable carbonation products could be attributed to this reaction.

Gypsum and ettringite were identified in the different mortars samples. Ettringite is a primary hydration product in Portland cement (reaction between the calcium aluminate and the sulfate form added gypsum) but rapidly dissolve after the sulfate depletion (first days of the cement hydration). This phase can precipitate again when external or internal sources of sulfate are available. In the present case, this mortar was applied on a column originally made of gypsum stone, continuously providing sulfate allowing ettringite to precipitate. Some Roman cements (American Rosendale RC, French Vicat and Vassy RC) are reported to contain sulfate phases [9,19] leading to the early formation of ettringite. However ettringite was identified only in the sample 3 (reprofiling mortar applied on the structural gypsum stone) while gypsum seems to be the common reaction products present within this series of samples.

3. Microstructure of the mortars by SEM

The microstructure of the mortar samples is illustrated in Figure 3 to Figure 5.
The main phases (typical to Portland cement) comprising a cement grain from sample 1 (Figure 3.a) were identified as C_3S (with Ca/Si= 3.15 ± 0.3), C_3A (with Al substituted by Fe, Ca/(Al+Fe) = 1.62 ± 0.02) and C_4AF (with Ca/Al = 2.09 ± 0.05 and Ca/(Al+Fe) = 1.16 ± 0.02). Note that C_3S was not identified by the XRD technique. The observation of this sample at lower magnification showed a many unreacted cement grains, suggesting a low degree of hydration. The nature of the hydration products (around the cement grains) is discussed below.
In sample 2 (Figure 3.b), three main phases were identified: C_2S (rich in Si with Ca/Si= 1.77 ± 0.2), C_2AS rich in Si, Ca/Si = 1.7 ± 0.16 and Ca/(Al+Si) = 0.76 ± 0.05) and the silica gel appearing in dark in the BSE images, at the boundary of the cement grain. While C_2S and C_2AS are common phases formed in Roman cement at relatively high temperature of calcination [14], the presence of the silica gel at the boundary can be considered as a weathering product of the cement exposed to atmospheric carbonation. This product results from the reaction between C_2S and CO_2, leading to the decalcification of C_2S and precipitation of silica gel, which would be a residual product of Ca depletion. This specific reaction is scarcely reported but the mechanism and the nature of the silicate polymer were recently studied on synthesized C_2S and Portland cement [20].

Figure 3-c shows another example of Roman cement grain in which only rounded C_2S grains were detected. Figure 3-d illustrates a Roman cement grain composed of C_2S surrounded by significant amounts of silica gel (as carbonation product of parent C_2S).

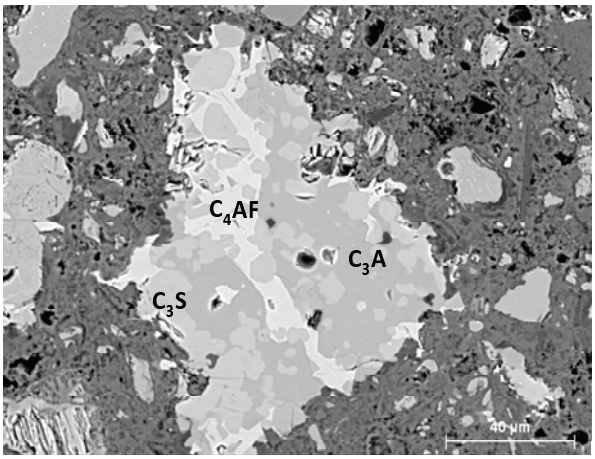

a: Sample 1

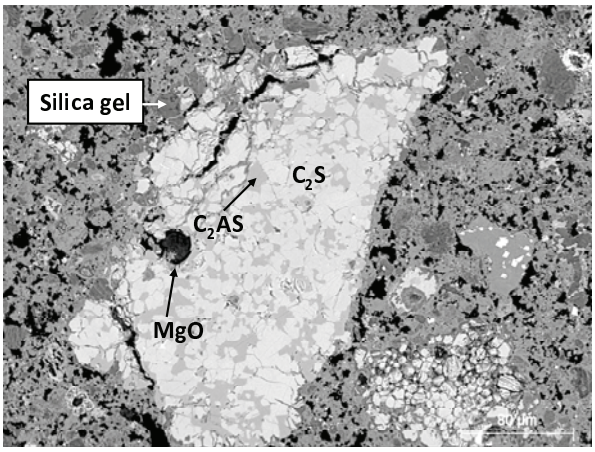

b: Sample 2

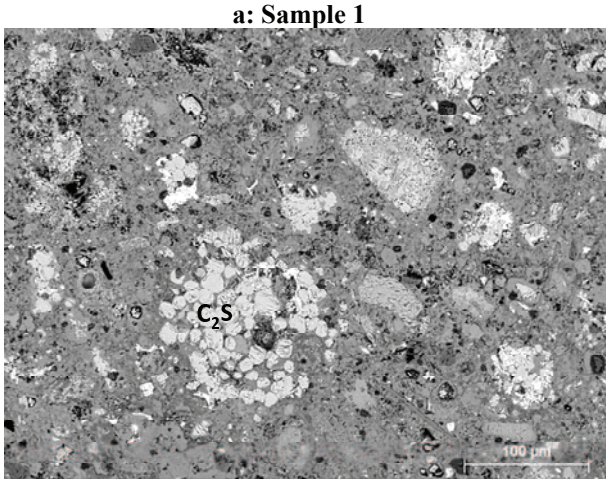

c: Sample 3

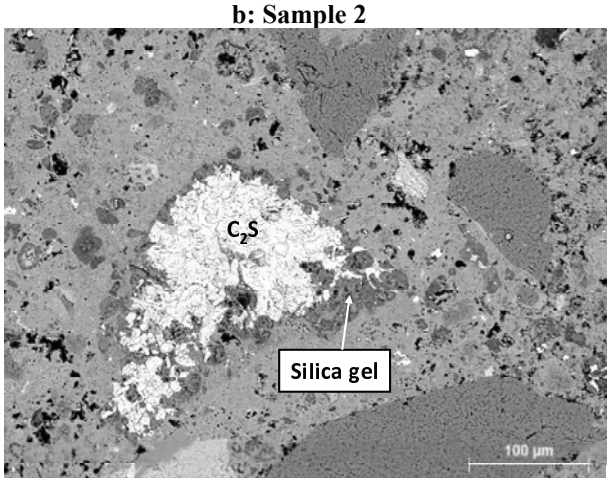

d: Sample 4

Figure 3 Main features of the cement grains

Figure 4 illustrates the microstructure of the samples 1 and 2 and gives the elemental composition (Ca, Al, Si, S, expressed in the atomic ratio graphs) of the hydration products. In the Portland cement mortar (sample 1), we distinguish typically two types of calcium silica hydrate, the inner C-S-H immediately surrounding the cement grains, and the outer C-S-H precipitated further in the microstructure. The latter are less dense and can incorporate other phases such as ettringite or monosulfoaluminate. The EDS dots distribution in the atomic ratio graph suggests that outer C-S-H is intermixed with both ettringite (Ett.) and/or monosulfoaluminate (Ms), while the latter was not detected by XRD, possibly because of their inherent poor crystallinity. The most important feature here lies in the comparison with the composition of the hydration products of the roman cement mortar (sample 2). First, no distinction between outer and inner products was observed in the hydrated binders. In addition, the atomic ratio graphs show a different phase assemblage than previously described. The distribution of Al, Ca and Si suggests that a C-A-S-H type phase intermixed with calcium carbonate dominates in the microstructure, with no clear evidence of a pure end-member C-S-H phase. The degree of carbonation of this sample is very high (e.g., the micrograph of Figure 4 show a cement grain with fully carbonated C_2S) which probably makes the analysis of outer hydration products difficult. However, recent studies on modern Roman cements [21] support the fact that C-S-H and CH, as hydration products of C_2S, are

not homogeneously distributed in the microstructure even after 90 days of hydration, in contrast to Portland cements.

The S/Ca *vs.* Al/Ca graph of the sample 2 shows that no sulphur bearing phase was detected, in the hydration products of the mortar.

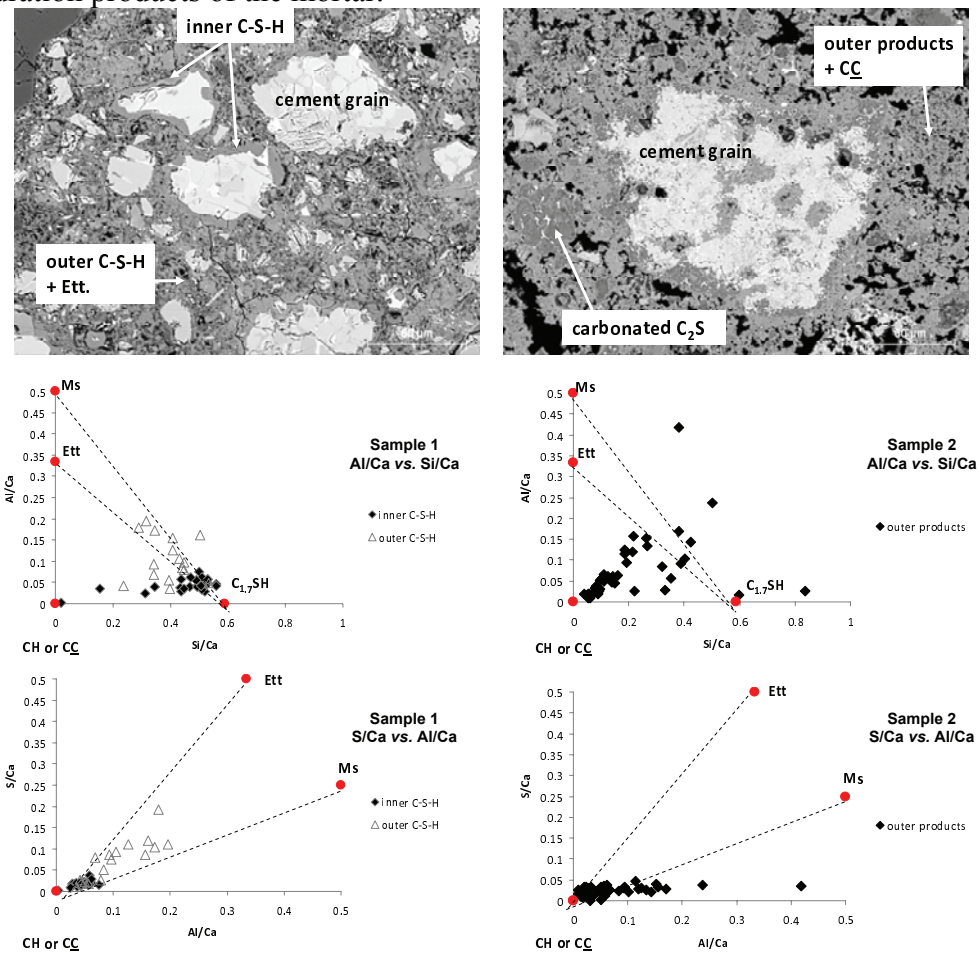

Figure 4 Microstructure and composition of hydration products, samples 1 and 2

The distribution of sulphur at the interface between the XIIth C. anhydrite mortar and the XIXth Roman cement mortar (sample 2) was studied by elemental mapping. Figure 5 shows a clear interface with no concentration gradient of sulphur at the boundary of the Roman cement mortar. Nonetheless sulphur may diffuse and few dot are visible in the Figure 5-b, which were attributed to the reaction between sulphur and CH to precipitate gypsum in the porosity.

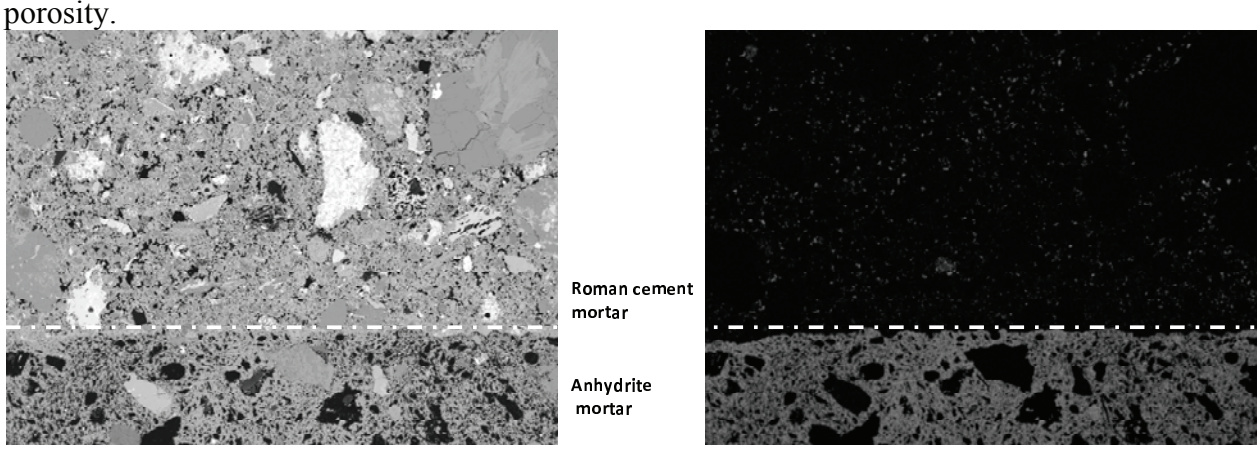

a: BSE image **b: Elemental distribution of sulfur**

Figure 5 Elemental mapping of the interface between anhydrite mortar and RC mortar (sample 2)

Figure 6 shows BSE images and the respective segmented grey level images that illustrate the distribution of the porosity (appearing in black) in the samples 2 and 4. In Figure 6- b and d, the pores resulting from mortar mixing are distinguished from the capillary porosity developed during the hydration of Roman cement. The network of the capillary pores is randomly distributed through the sample, allowing soluble sulphur to migrate and calcium suphate (or ettringite) to precipitate in available space. This provides to Roman cement mortars some specific transfer properties adapted to the substrates (here, anhydrite mortar or gypsum stone).

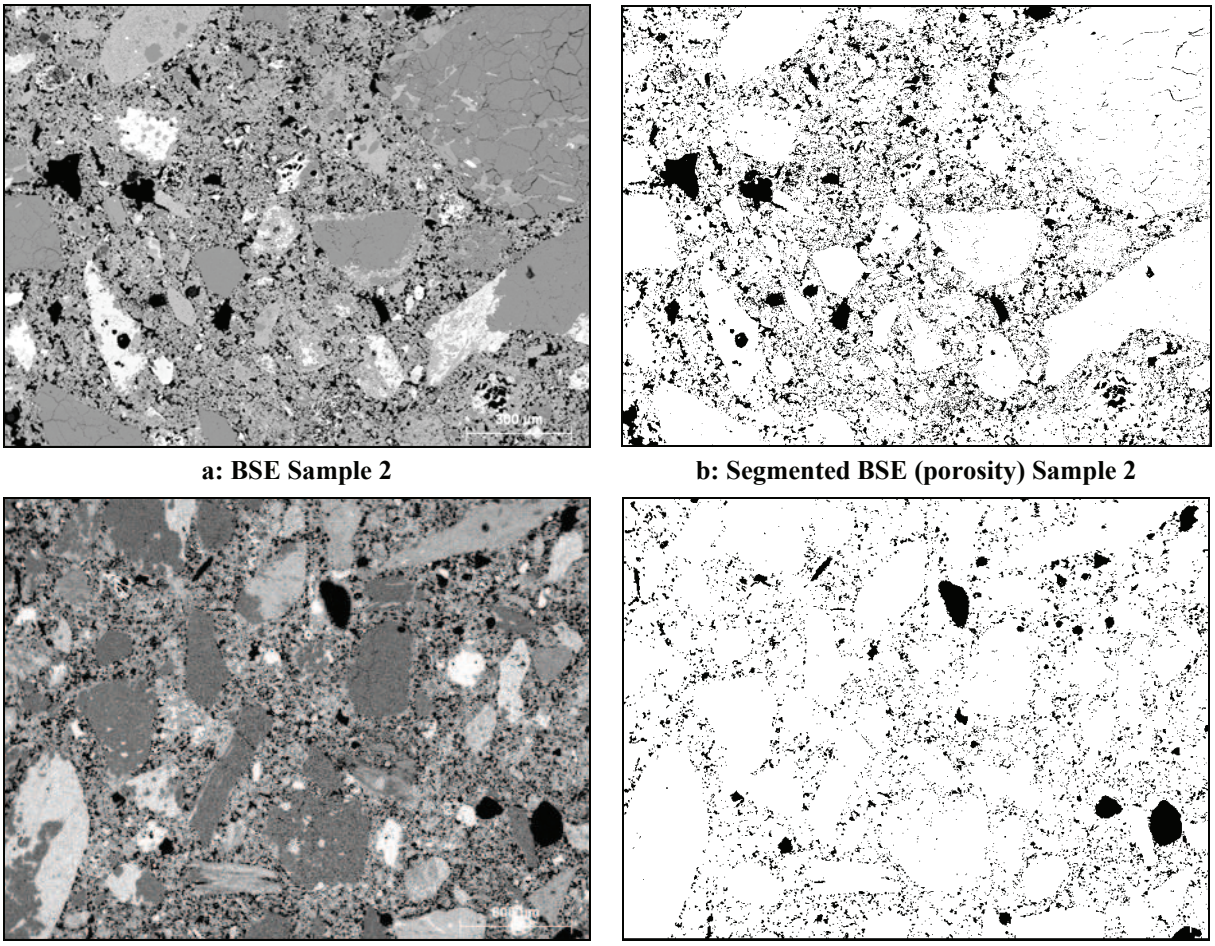

a: BSE Sample 2 **b: Segmented BSE (porosity) Sample 2**

c: BSE Sample 4 **d: Segmented BSE (porosity) Sample 4**

Figure 6 BSE images of samples 2 and 4 (a and c) and segmentation of grey level: distribution of the porosity in the samples 2 and 4 (b and d)

5. Conclusions

The use of Roman cement mortars in the late XIXth C. on the façades of the church of Valere (Sion, CH) was presented. The specific application as joints of structural gypsum stones and render of earlier mortar made of anhydrite was discussed. Roman cement belongs to a specific family of hydraulic binders developed during the XVIIIth C and which shows interesting compatibility properties adapted to stone conservation.

The samples show a grade of cement containing significant amounts of unreacted gehlenite and β-C_2S, suggesting a calcination process using a temperature range above 1000°C, likely that of the French Vicat cement and higher than typically reported for Roman cements (800-1000°C). Recent studies showed that the microstructure development of hydrated modern Roman cements is controlled by dissolution of amorphous CaO-Al_2O_3 and fine calcium

carbonate (both from the raw cement) and precipitation of carbonated phases in the CaO-Al_2O_3-CO_3-H_2O system. If sulphur is present in the raw cement, ettringite and monocarboalumiante precipitate, as in the case of the French Vicat cement containing gypsum [19,21]. These elongated crystals (plate of carbonated phases or ettringite needles) precipitate very rapidly to form a poorly packed microstructure in the first minutes of hydration. However, this phase assemblage develops minimal strength, allowing the rapid application of mortars for cast elements or renders. This microstructure becomes progressively and locally denser after the later reaction of calcium silicate (mainly α'-C_2S but also β-C_2S for the cements produced at higher temperature) forming, in theory, C-S-H and CH. However the presence and location of these two phases in hydrated Roman cement remains difficult to identify in contrast to the case of C_3S hydration in Portland cements. This identification becomes more challenging in highly carbonated samples, where different calcium carbonate polymorphs are uniformly distributed in the primary hydration products. Carbonation acts also on the non reacted C_2S, during which decalcification leads to the formation of silica gel at the cement grain boundary. This reaction may contribute to the reduction of the extent of C_2S dissolution and cement hydration.

The excellent state of conservation of Roman cement mortar could be explained by its microstructure and the high capillary porosity developed during hydration [22,23]. This allows the sulphur, dissolved from the gypsum stone, to migrate through the Roman cement mortar and to potentially react to form gypsum (or ettringite in sample 3) without generating internal stress and subsequent cracks formation. This specific feature is one of the most important characteristics that make Roman cements highly suitable as a restoration mortar in contrast to the Portland cement mortar that was inappropriate for replicating a window column originally made of gypsum stone.

6. Acknowledgements

The European Project ROCARE is acknowledged for the financial support of this case study. The architect C. Amlser is also gratefully acknowledged for his interest in this material and the current opportunity to use the Church façade as a demonstration site for modern Roman cement mortar applications. CG would like to dedicate this paper to the memory of Pr. Michele Coutant, her knowledge and her passion of the conservation of cultural heritage.

7. References

[1] Raemy-Berthod, C., 2003. Inventaire suisse d'architecture, 1850-1920: Sion. *Société d'Histoire de l'Art en Suisse* 9 92.

[2] Winkler, E.M., 1997. *Stone in Architecture: Properties, Durability*. Springer

[3] Regourd, M., Kerisel, J., Deletie, P. and Haguenauer, B., 1988. Microstructure of mortars from three Egyptian pyramids. *Cement and Concrete Research* 18 (1) 81-90.

[4] Cotrim, H.l., Veiga, M.d.R.r. and de Brito, J., 2008. Freixo palace: Rehabilitation of decorative gypsum plasters. *Construction and Building Materials* 22 (1) 41-49.

[5] Luxan, M.P., Dorrego, F. and Laborde, A., 1995. Ancient gypsum mortars from St. Engracia (Zaragoza, Spain): Characterization. Identification of additives and treatments. *Cement and Concrete Research* 25 (8) 1755-1765.

[6] Livingston, R.A., A. Wolde-Tinsae and Chaturbahai, A., 1991. The Use of Gypsum Mortar in Historic Buildings. In: C. Brebbia, *Structural Repair and Maintenance of Historic Buildings*, Southampton UK,

[7] Adams, J., Kneller, W. and Dollimore, D., 1992. Thermal analysis (TA) of lime- and gypsum-based medieval mortars. *Thermochimica Acta* 211 (0) 93-106.

[8] Weber, J., Gadermayr, N., Bayer, K., Hughes, D., Kozlowski, R., Stillhammerova, M., Ullrich, D. and Vyskocilova, R., 2008. Roman cement mortars in Europe's architectural heritage of the 19th century. *ASTM Special Technical Publication*, 69-83.

[9] Gosselin, C., Verges-Belmin, V., Royer, A. and Martinet, G., 2009. Natural cement and monumental restoration. *Materials and Structures/Materiaux et Constructions* 42 (6) 749-763.

[10] Hughes, D.C., Swann, S. and Gardner, A., 2007. Roman cement: Part one: Its origins and properties. *Journal of Architectural Conservation* 13 (1) 21-36.

[11] Avenier, C., Rosier, B. and Sommain, D., 2007. *Ciment naturel*. Glénat

[12] Werner, D. and Burmeister, K., 2007. An Overview of the History and Economic Geology of the Natural Cement Industry at Rosendale, Ulster County, New York. *Journal of ASTM International* 4 (6) 14.

[13] Dariz, P., 2009. Romanzement in der Schweiz – Geschichte des natürlich hydraulischen Bindemittels in der Eidgenossenschaft. *Restauro* 8 8.

[14] Hughes, D.C., Jaglin, D., Kozlowski, R. and Mucha, D., 2009. Roman cements - Belite cements calcined at low temperature. *Cement and Concrete Research* 39 (2) 77-89.

[15] Hughes, D.C., Jaglin, D., Kozlowski, R., Mayr, N., Mucha, D. and Weber, J., 2007. Calcination of marls to produce Roman cement. *Journal of ASTM International* 4 (1)

[16] Pinter, F., *personnal communication*: Vienna.

[17] Campbell, D.H., 1999. *Microscopical examination and interpretation of portland cement and clinker*. Portland Cement Association

[18] Thiery, M., Villain, G., Dangla, P. and Platret, G., 2007. Investigation of the carbonation front shape on cementitious materials: Effects of the chemical kinetics. *Cement and Concrete Research* 37 (7) 1047-1058.

[19] Vyskocilova, R., Schwarz, W., Mucha, D., Hughes, D., Kozlowski, R. and Weber, J., 2008. Hydration processes in pastes of Roman and American natural cements. *ASTM Special Technical Publication*, 96-104.

[20] Shtepenko, O., Hills, C., Brough, A. and Thomas, M., 2006. The effect of carbon dioxide on β-dicalcium silicate and Portland cement. *Chemical Engineering Journal* 118 (1-2) 107-118.

[21] Gosselin, C., Scrivener, K.L. and Feldman, S.B., 2011. Microstructure of roman cements used for architectural restoration. *International Conference on Cement Chemistry*, Madrid,

[22] Klisinska-Kopacz, A., Tislova, R., Adamski, G. and Kozlowski, R., 2010. Pore structure of historic and repair Roman cement mortars to establish their compatibility. *Journal of Cultural Heritage* 11 (4) 404-410.

[23] Bayer, K., Gosselin, C., Hilbert, G. and Weber, J., 2011. Microstructure of historic and modern Roman cements to understand their specific properties. In: T.K. Alenka Mauko, Tinkara Kopar, Nina Gartner, *13th Euroseminar On Microscopy Applied To Building Materials*, Ljubljana, 2-3.